

# Plasmon effect of graphene quantum dots on corrugated silver film

## Abstract

Graphene quantum dots were prepared successfully, and their characteristics identified by Raman spectra and HR-TEM. In addition, the absorption and photoluminescence were studied for their optical properties. The Raman scattering effects were studied for graphene quantum dots (GQDs) coupling with the corrugated structure silver (Ag) films. The corrugated silver films were prepared by evaporating metallic Ag on opal crystal substrates. The opal crystal substrates were fabricated from 600nm SiO<sub>2</sub> spheres. The intensity enhancement of photoluminescence and Raman spectral bands of the GQDs on the corrugated Ag films was observed and explained. Study of Raman spectra showed the surface-enhanced Raman scattering effect.

**Keywords:** graphene quantum dots, opal crystal, plasmonic, sers, photoluminescence

Volume 2 Issue 6 - 2018

Pham Nam Thang,<sup>1,2</sup> Le Xuan Hung,<sup>2,3</sup> Vu Duc Chinh,<sup>1</sup> Phan Ngoc Hong,<sup>1,2</sup> Duong Ngoc Tu,<sup>4</sup> Pham Thu Nga<sup>1,2,3</sup>

<sup>1</sup>Institute of Materials Science, Vietnam Academy of Science and Technology, Vietnam

<sup>2</sup>Graduate University of Science and Technology, Vietnam Academy of Science and Technology, Vietnam

<sup>3</sup>Institute of Research and Development, Duy Tan University, Vietnam

<sup>4</sup>Institute of Chemistry, Vietnam

**Correspondence:** Pham Nam Thang, Institute of Materials Science, Vietnam Academy of Science and Technology, 18 Hoang Quoc Viet Road, Cau Giay District, Hanoi, Vietnam, Email [thangpn@ims.vast.vn](mailto:thangpn@ims.vast.vn)

**Received:** December 01, 2017 | **Published:** December 31, 2018

**Abbreviations:** GQDs, graphene quantum dots; SERS, surface enhanced raman scattering; SPP, surface plasmon polariton; CFGs, chemical functional groups

## Introduction

Graphene quantum dots (GQDs) with highly tunable properties are attracting interest from researchers. Their potential applications are biosensor, light emitting diodes, displays, solar cells, super capacitors, transistors, photo catalysts, drug delivery and medical imaging.<sup>1,2</sup> In this study, we have used the bottom up method to fabricate GQDs by a simple and safe method that is able to mass produce, from two different initial precursors: citric acid (CA) and pyrene. The information on the structure of fabricated GQDs was all studied with micro-Raman spectra combined with TEM and HR-TEM image recording. The combination of GQDs with convexing metal surfaces to increase intensity of optical signals such as absorption, emission or Raman scattering is a very interesting concept and would lead to many practical applications in solar cells or biosensors. In order to take advantage of surface plasmon polariton (SPP) modes, which are not coupled to far-field radiative modes in the case of a planar metallic surface, many studies have introduced a periodic corrugation to the metallic surface.<sup>3</sup> The main idea of this study is to use thin films of corrugated 2D Ag layers with organized structure - thanks to the coverage of Ag on top of an opal structure created from SiO<sub>2</sub> spheres - to apply in enhancing the optical signals of GQDs.<sup>4</sup> In order to cover the Ag layer on opal, we have fabricated a hundred grams of 600nm SiO<sub>2</sub> spheres with narrow size distribution. These opal samples were used as a periodic template for the fabrication of opaque two-dimension corrugated metallic grating. The emission and Raman spectra of GQDs are put on the Ag periodic corrugated film samples covering the opal surfaces are also carried out. This study bring the idea for the potential applications in nano antenna and biosensor.

## Materials and methods

### Synthesis of graphene quantum dots from citric acid and pyrene

Synthesize GQDs from citric acid (CA): The GQDs were prepared by hydrothermal treatment of citric acid (Fisher, 95.5%) as reported.<sup>5</sup> In a typical synthesis, 5mmol CA and 15mmol urea (Aldrich) were dispersed in 25ml of water under stirring to form clear solution then transferred into a 100 ml Teflon lined stainless autoclave. The reaction samples were kept for 4 hours at temperatures from 160°C up to 200°C and denoted G1. After cooling to room temperature, the GQD product was collected by adding ethanol into the solution and centrifuged at 5000rpm for 5 min, call G1.

Synthesize GQDs from pyrene : The used synthesis method was reported.<sup>2</sup> In a typical procedure for synthesis of OH-GQDs, pyrene (2g, purity 98%, HPLC) was nitrated into trinitropyrene in hot HNO<sub>3</sub> (160ml, 68%) at 80°C under refluxing and stirring for 12h. The mixture was diluted with deionized (DI) water (1 l) and filtered through a 0.22mm microporous membrane to remove the acid. The resultant yellow 1,3,6-trinitropyrene was dispersed in an NaOH 0.2M solution of DI 600ml water by ultrasonication for 2h. The suspension was transferred to a Teflon-lined autoclave and heated at 200°C for 10h. The product containing water-soluble GQDs was filtered through a 0.22mm membrane to remove insoluble carbon products. The GQD product, called G2, was collected by adding ethanol into the solution and centrifuged at 5000rpm for 5 min with 3 times repeat in order to remove all sodium salt. All the purified GQDs were dried or re-dispersed into water for further characterization and use.

### Fabrication of metallic Ag films on the periodic template of opal

Preparation of SiO<sub>2</sub> spheres with large-scale and metallic Ag films

on the periodic template of opal with calculated Ag thickness are presented in previous publication.<sup>6</sup> Ag films are fabricated by thermal evaporating an Ag layer on a self-assembled periodical array of opal with different Ag thickness. In this study, the 135nm Ag layer films were chose for dispersing GQDs on the convexing surface to form their combination with the Ag plasmonic surface can be observed.

Characterization of the samples: The purified GQD samples were used to measure HR-TEM. Field emission scanning electron microscope (FE-SEM)-S4800-Hitachi to determine the size of SiO<sub>2</sub> spheres, morphology of the opal samples and Ag layer thickness on opal. The absorption spectra were measured by Cary 5000 UV-Vis-NIR (Aligent Technologies, US). The PL spectra measurement was carried out on a Fluorolog-322 system (Jobin-Yvon). The GQDs samples were analyzed by Micro Raman spectroscopy (XploRA-Horiba).

## Results and discussion

In this part, we present the results on identification of GQDs fabricated and their relevant characteristics. The GQDs were dispersed on the convexing surface of the Ag film so that their combination with the Ag plasmonic surface can be observed by presenting the increased intensity of vibration line from Raman spectra. Raman Characterization of Prepared GQDs. Raman spectra of GQDs: Raman spectra are showed in the Figure 1 for identify the structure formation of GQD samples G1 and G2. The G band is a first-order scattering process that originates from the double-degenerate vibrational mode ( $E_{2g}$ ) that occurs at the crossing of the longitudinal optical (LO) and transverse optical (TO) phonon branches at the  $\Gamma$  point in the first Brillouin zone of graphene.<sup>7,8</sup> In addition to the peaks identified in the spectra, we now also observe the defect-induced D band. Due to momentum conservation, the TO phonons giving rise to this band only become Raman active if the electrons or holes involved in the scattering process undergo elastic scattering by a lattice defect which in this case is provided by the graphene edge.<sup>9,10</sup>

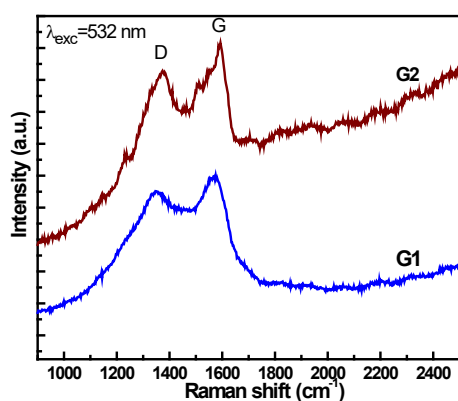


**Figure 1** Raman spectra of GQD samples G1 and G2 were prepared by two different methods.

Two peaks D and G are both clearly observable on Raman spectra, however the intensity ratio (ID/IG) is different depending on the fabrication method. The samples G1 and G2 have the ID/IG ratio of 1.07 and 1.05, respectively, which is similar to the GQDs fabricated by the hydrothermal method.<sup>2,11,12</sup> The D peak of the Raman spectrum comes from the “unorganized” carbon<sup>8,13</sup> which is associated with the defects or the edges of graphene. In our samples, the high D peak should result from the high ratio of graphene edge in GQDs. However,

it should be mentioned here that the GQDs synthesized by a solution process could get a much lower ID/IG<sup>14</sup> due to edge passivation of the chemical functional groups (CFGs) as an observable case for samples G1. We could not observe the frequency band where the 2D peak might have appeared. It is because the 2D peak of GQDs is about one third of the G peak, indicating that the GQDs consist of a few atomic layers. The position of G peak is relevant to the number of layers in the GQD sample.<sup>15</sup> This position on the Raman spectra of GQD samples in this study is all at frequencies longer than 1593cm<sup>-1</sup> compared to 1582cm<sup>-1</sup> of single-crystalline GQDs published.<sup>2</sup> Therefore it can be assumed that G2 sample (fabricated from pyrene) have more than just a single layer. For sample G1 fabricated from CA precursor, the G peak is positioned at 1572cm<sup>-1</sup>, lower than that published.<sup>2</sup> Thus, it is difficult to conclude on the number of layers existing in GQD samples based on only Raman spectra results, because the data on G peak positions differ in different publications.

## HR-TEM images

Fabricated GQD samples were also studied in shape and size with TEM images. Figure 2 & Figure 3 are the TEM images with the scale bar of 10 nm for the sample fabricated from citric acid with average size of about 15 nm and the scale bar of 20nm for the sample G2. The Figure 3 shows HR-TEM image of the lattice spacing distance  $d$  is 0.24 nm. From the analysis results of the sample's characteristics with micro-Raman spectra and HR-TEM images, it can be concluded that the fabricated sample has round shape and is GQDs.

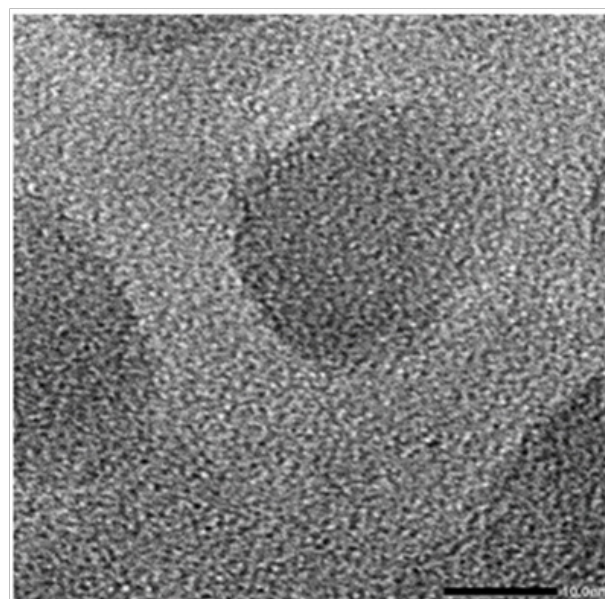


**Figure 2** HR-TEM image of the GQD sample fabricated from citric acid, scale bar: 10nm.

Absorption and emission spectra: The absorption spectra of two samples fabricated from CA and pyrene were presented in Figure 4.

The spectra usually show a prominent peak at  $\approx 230$ nm, assigned to the  $\pi-\pi^*$  excitation of aromatic sp<sup>2</sup> domains<sup>16</sup> and a large absorption band is positioned at about 334 nm and 374 nm. The excitonic absorption band centered at about 334nm and an optical absorption edge at  $\sim 425$ nm (or  $\sim 500$ nm) depending on the sample. The position of the peak depends on the size and edge status of each sample. Therefore, it can be seen that these samples can all absorb light in the UV. The luminescence properties of GQDs are strongly dependent on

the synthesis method. Thus, the mechanism of GQD luminescence is still disputable, and a new way to synthesize CFGs-free GQDs is crucial for deeply understanding the origin of GQD luminescence.

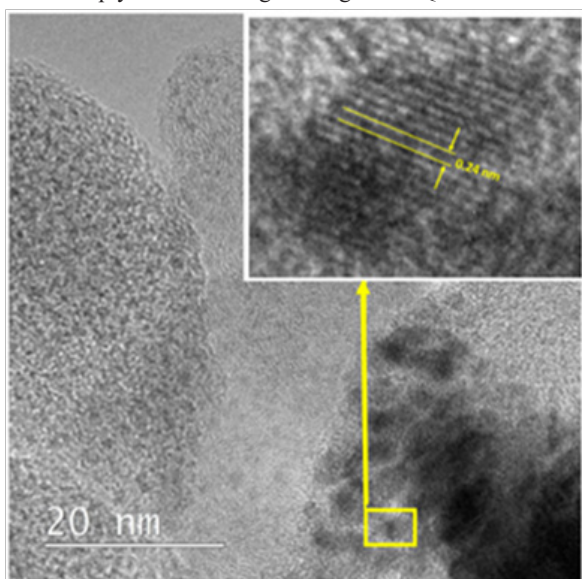


Figure 3 HR-TEM image of GQD sample fabricated from pyrene, scale bar: 20nm.

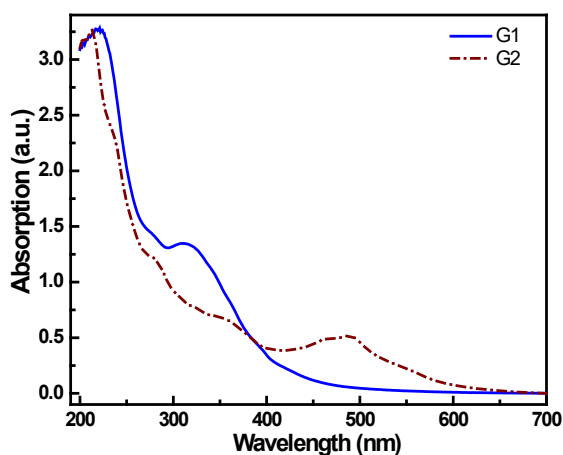


Figure 4 Absorption spectra of the GQDs samples prepared from citric acid (G1) and pyrene (G2).

Figure 5 shows the emission spectra of 2 different GQD samples fabricated from CA (G1) and pyrene (G2) under the same excitation wavelength of 365nm. Their emission spectrum is a broad band with maximum peak barely changes 447nm for sample G1 (blue region) and 530nm (green region) for sample G2. The general comment is that samples fabricated from CA all emit under UV light, and emit stronger when GQD samples are diluted. These fabrication methods only produce GQD samples with low concentration. In contrast, samples fabricated from pyrene allow fabrication of GQD with high concentration. These GQD samples have a black colour after filtering redundant substances post fabricating reaction. The proposed PL mechanism based on the emissive free zigzag sites is further supported by the observed pH-dependent PL reported.<sup>12</sup> Thus, we can say that the blue luminescence may originate from free zigzag sites of GQDs. The GQDs emit strongly following the mechanism related to defect sites on the edge.

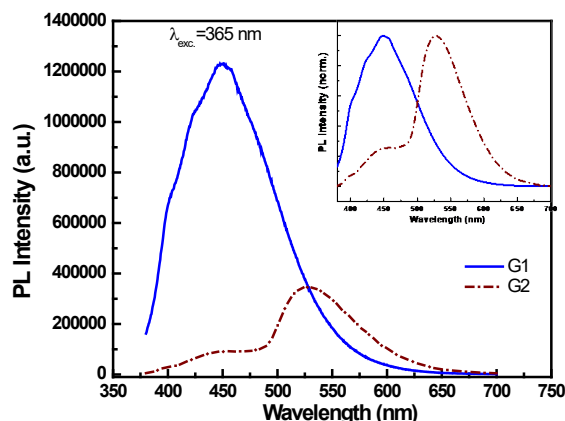


Figure 5 Emission spectra of the GQDs samples excited by  $\lambda_{exc} = 365$  nm. Inset is norm. PL spectra of G1 and G2.

Raman spectra of GQDs combined with periodically corrugated Ag film. Figure 6 shows the Raman spectra of GQDs (G1) on convexing film with 135nm Ag thickness, on Ag flat and on glass. The Raman spectra of GQDs on convexing Ag films with 135 thickness immediately show the strong increase in intensity of vibration lines D and G, compared to those measured on Ag flat and on glass. This line intensity increases 5 times compared to GQDs samples measured on Ag flat and up to 36.3 times compared to the case on glass, respectively, with the same condition. The significant Raman enhancement of GQDs on the Ag periodic corrugated opal film are also observed at the peaks located before  $3000\text{cm}^{-1}$ . The strong increase in vibration line intensity can be explained as due to the presence of the surface-plasmon-polariton modes.

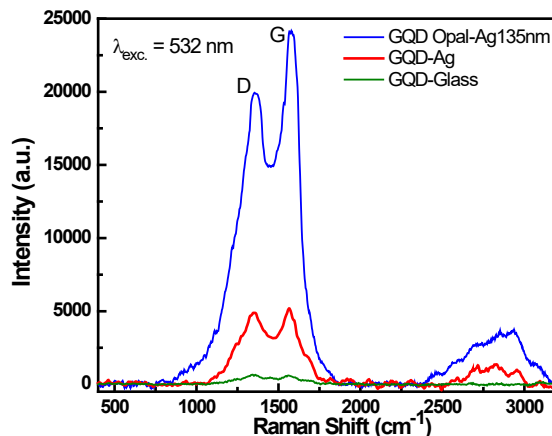


Figure 6 The Raman scattering spectra of GQD (G1) on the Ag coating opal substrate, GQD on Ag flat film and GQDs on glass substrate. The excitation wavelength is 532nm.

### Conclusion

In summary, we have fabricated GQDs with identifying characteristics that are the distance between inter-planes determined by experiment from HR-TEM image,  $d=0.24\text{nm}$ . Using citric acid precursor can produce GQDs with strong emission but low particle concentration, and using pyrene can produce GQDs with higher concentration that emit easily in green region. Raman measurements have allowed the identification of samples as GQDs. The studies on the combination of the emission of GQDs with these Ag films have

been done. The enhanced Raman scattering effect with the surface-plasmon-polariton modes was observed for the corrugation Ag sample with 135nm thickness for all these GQDs.

## Acknowledgments

This research is funded by Project: VAST. HTQT. PHAP. 01/15-16 and by project CSLC 04.17 of Institut of Materials Science of VAST. The authors thank the National Key Laboratory for Electronic Materials and Devices- IMS and Duy Tan University for the use of facilities. We would like to thank Dr. Masaki Tanemura of Nagoya Institute of Technology, Graduate School of Engineering, Nagoya, Japan for the help.

## Conflicts of interest

The author declares there is no conflicts of interest.

## References

1. Sora Bak, Doyoung Kim, Hyoyoung Lee. Graphene quantum dots and their possible energy applications: A review. *Current Applied Physics*. 2016;16(9):1192–1201.
2. Wang L, Wang Y, Xu T, et al. Gram-scale synthesis of single-crystalline grapheme quantum dots with superior optical properties. *Nat Commun*. 2014;5:5357.
3. Frederich H, Wen F, Laverdant J, et al. Isotropic broadband absorption by a macroscopic self-organized plasmonic crystal. *Opt Express*. 2011;19(24):24424–24433.
4. C Lethiec, G Binard, T Popescu, et al. Plasmonics of Opal Surface: A Combined Near- and Far-Field Approach. *The Journal of Physical Chemistry C*. 2016;120:19308–19315.
5. Yongqiang Dong, Jingwei Shao, Congqiang Chen, et al. Blue luminescent graphene quantum dots and graphene oxide prepared by tuning the carbonization degree of citric acid. *Carbon*. 2012;50(12):4738–4743.
6. Pham Nam Thang. Large-scale synthesis of 600nm-sized SiO<sub>2</sub> spheres with narrow size distribution, fabrication of opal crystal films from these SiO<sub>2</sub> spheres and Ag plasmonic crystal thin-films on top as substrate in biosensors. *IWAMSN*. 2016;286–292.
7. R Beams, LG Cancado, L Novotny. Low temperature Raman study of the electron coherence length near graphene edges. *Nano let*. 2011;11(3):1177–1181.
8. F Tuinstra, JL Koenig. Raman Spectrum of Graphite. *J Chem Phys*. 1970;53(3):1126.
9. LG Cancado, MA Pimenta, BR Neves, et al. Influence of the atomic structure on the Raman spectra of graphite edges. *Physical review letters*. 2004;93(24):247401.
10. LG Cancado, R Beams, L Novotny. Optical Measurement of the Phase-Breaking Length in Graphene. *Laser science*. 2010.
11. Kun Huang, Wanglin Lu, Xuegong Yu. Highly Pure and Luminescent Graphene Quantum Dots on Silicon Directly Grown by Chemical Vapor Deposition. *Particle & Particle Systems Characterization*. 2016;33(1):8–14.
12. D Pan, J Zhang, Z Li, et al. Hydrothermal route for cutting graphene sheets into blue-luminescent graphene quantum dots. *Adv Mater*. 2010;22(6):734–738.
13. Ferrari AC, Meyer JC, Scardaci V, Raman spectrum of graphene and graphene layers. *Phys Rev Lett*. 2006;97(18):187401.
14. Li Y, Hu Y, Zhao Y, et al. An electrochemical avenue to green-luminescent graphene quantum dots as potential electron-acceptors for photo voltaics. *Adv Mater*. 2011;23(6):776–780.
15. Tang L, Ji R, Cao X, et al. Deep Ultraviolet Photoluminescence of Water-Soluble Self-Passivated Graphene Quantum Dots. *ACS Nano*. 2012;6(6):5102–5110.
16. Wang R, Shang Y, Kanjanaboos P, et al. Colloidal quantum dot ligand engineering for high performance solar cells. *Energy Environ Sci*. 2016;9(4):1130–1143.